PERGAMON

International Journal of Solids and Structures 40 (2003) 6981–6988

INTERNATIONAL JOURNAL OF SOLIDS and STRUCTURES

www.elsevier.com/locate/ijsolstr

On the performance of truss panels with Kagomé cores

J. Wang [a], A.G. Evans [a,*], K. Dharmasena [b], H.N.G. Wadley [b]

[a] *Department of Mechanical and Aerospace Engineering, Princeton University, Princeton, NJ 08544, USA*
[b] *Department of Materials Science and Engineering, University of Virginia, Charlottesville, VA 22903, USA*

Received 17 September 2002

Abstract

The performance characteristics of a truss core sandwich panel design based on the 3D Kagomé has been measured and compared with earlier simulations. Panels have been fabricated by investment casting and tested in compression, shear and bending. The isotropic nature of this core design has been confirmed. The superior performance relative to truss designs based on the tetrahedron has been demonstrated and attributed to the greater resistance to plastic buckling at the equivalent core density.

Keywords: Truss core panels; 3D Kagomé; Isotropy; Plastic buckling resistance; SEM

1. Introduction

Recent assessment of ultra-light metallic systems has revealed that periodic truss core panels exhibit superior thermo-structural characteristics (Wicks and Hutchinson, 2001; Wallach and Gibson, 2001; Deshpande et al., 2001; Evans et al., 2001; Deshpande and Fleck, 2001; Chiras et al., 2002). The preferred core topologies are those that stretch/compress without bending. The properties of such cores are linearly related to relative density (Wicks and Hutchinson, 2001; Wallach and Gibson, 2001; Deshpande et al., 2001; Evans et al., 1998, 2001; Deshpande and Fleck, 2001; Chiras et al., 2002) and the panels are at least as weight efficient as the best competing concepts (Evans et al., 1998). Two such topologies have been analyzed and characterized experimentally: tetrahedral (Deshpande and Fleck, 2001; Chiras et al., 2002) and pyramidal (Deshpande and Fleck, 2001). The shear and compressive response of these cores has been determined, and the superior bending characteristics of panels affirmed in near-optimized configurations (Chiras et al., 2002; Evans, 2001). Nevertheless, topologies with even better performance appear feasible. One such topology has been designated the 3D Kagomé core (Fig. 1). The performance of this topology has been explored by the finite element simulations presented in the companion article (Hyun et al., 2002). The results indicate advantages over other cores, primarily because of superior isotropy and greater resistance to softening modes (such as plastic buckling). The purpose of the present article is to design, fabricate and

* Corresponding author. Fax: +1-609-258-1177.

0020-7683/$ - see front matter © 2003 Published by Elsevier Ltd.
doi:10.1016/S0020-7683(03)00349-4

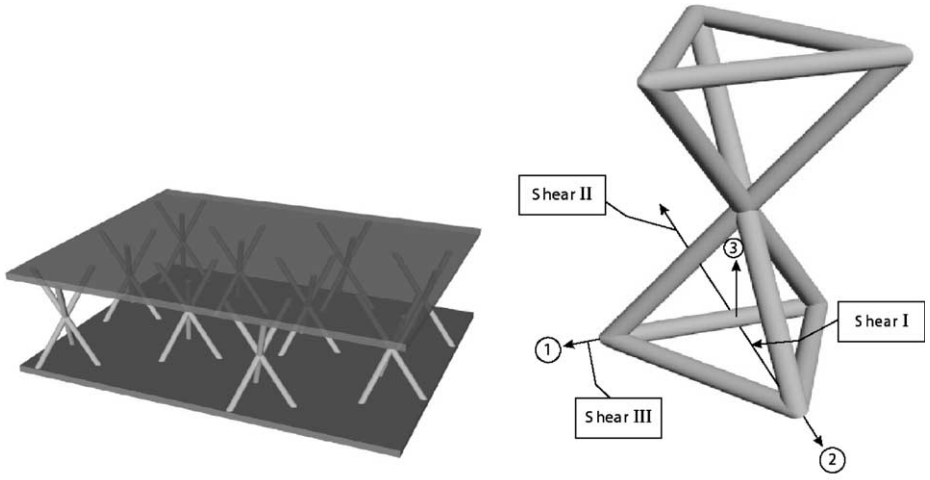

Fig. 1. (a) A truss core panel with solid face sheets and 3D Kagomé core. (b) A unit cell of the 3D Kagomé core: the truss diameter is about twice that for the optimized configuration.

measure the performance of Kagomé core sandwich panels with solid face sheets. Comparisons with simulated responses (Hyun et al., 2002) are used to establish the performance attributes of this topology.

2. Experimental design

To facilitate comparison with previous numerical results (Hyun et al., 2002), as well as with measurements performed on panels with tetrahedral cores (Chiras et al., 2002), the panels were fabricated by investment casting, using a copper/beryllium casting alloy (Cu–2%Be). The basic stress/strain behavior of this alloy has been characterized (Chiras et al., 2002). The dimensions of the core have been chosen to be representative of near-optimal sandwich panels (Wicks and Hutchinson, 2001; Chiras et al., 2002), with thicker-than-optimum faces to resist puncturing. Accordingly, the relative core density is 2% and the face sheets are about seven times thicker than the optimal. To attain a relative core density equal to that used in the previous tests (Chiras et al., 2002), the truss length is half that for the tetrahedral design. Each core element is separated from its nearest neighbors by a distance equal to the length of the base, as indicated on Fig. 1.

3. Panel fabrication

The complexity in fabrication of the truss core increases considerably from a 2D corrugated truss to a 3D Kagomé architecture. One option is to use injection molding to create a wax or polymer template of the truss core that can be used as a sacrificial pattern for investment casting. This however requires the fabrication of an intricate and often expensive die. Furthermore, if a design change in the sandwich panel has to be made, a new die has to be made with additional costs. The rapid prototyping approach offers a less expensive and far more flexible design and manufacturing option. Since the basis of any rapid prototyping technique is a computer generated three-dimensional solid model of the object, it provides the convenient creation of sandwich panels of optimal, near optimal, and sub-optimal designs for performance compar-

isons. The different panels can be created by varying the geometric parameters of the design features (e.g. face sheet thickness, core member diameter, core member length, panel size).

An extrusion based fused deposition modeling process commercialized by Stratasys Inc., Eden Prairie, Minnesota was selected as the rapid prototyping approach to make acrylonitrile butadiene styrene (ABS) sandwich panels with the Kagomé design. In this method, the 3D computer generated model was converted to a series of 2D layered tool path data using a proprietary mathematical slicing algorithm. The ABS model material was extruded from a nozzle through a fine tip and deposited along paths tracing the shape of the object. A second nozzle extruded an ABS soluble release material to provide a support structure for the core members. The part was built from bottom up to create the three-dimensional sandwich panel. Panels with core member diameters of 1.25 mm were constructed with an overall panel size of $246\times66\times14.4$ mm. The face sheet thickness and core member length were kept constant at 1.5 and 14 mm respectively. The overall panel size was selected to accommodate 10 cells in the length direction and four cells in the width direction similar to panels fabricated previously with the octet truss configuration (Chiras et al., 2002). Upon removal of each panel from the rapid prototyping machine, the support structure was dissolved by placing the parts in a soluble concentrate and water solution at 70 °C, and when dry, a coat of clear acrylic was sprayed to improve the surface finish of the ABS panels.

The rapid prototyped ABS patterns were supplied to Precision Microcast Inc. for investment casting in a Cu–2%Be alloy. The patterns were cleaned with isopropyl alcohol and coated with a liquid wax. A multiple gating system and a runner system (connecting the gates) were attached to the ABS pattern in casting wax along with three vent channels. The patterns were then subjected to several dips in a ceramic slurry followed by coatings of fine to medium grain zircon or fused silica while allowing to air dry in between each ceramic coating layer. Six to seven layers were allowed to form to build up sufficient strength in the ceramic shell. (The exact details of the process have been reported elsewhere (Chiras et al., 2002).) The ceramic coated tips of the vent channels were then ground to expose the ABS and allow gases to escape during the ABS burnout process which was carried out in a furnace at a temperature of 1066 °C for 1.5 h.

After the burnout process, the residual ash was removed from the hollow ceramic shell by rinsing with water and with the application of a high-pressure air jet. The vent channels were re-plugged with refractory cement and the ceramic shells preheated to 980 °C in preparation for pouring. The copper beryllium alloy was induction melted in a 14 kg crucible and poured into the ceramic mold at a temperature of 1425 °C. When the shells had cooled, the sandwich panel casting with the attached gating and runner system was retrieved by using a high-pressure water jet on the outer ceramic shell. The runners and gates were cut off and ground flush with the face sheet surfaces and residual material within the truss core region was removed by sandblasting.

4. Measurements

4.1. Compression

To measure the compressive response, the bottom face sheet was rigidly attached to a base plate and forces applied to the top face within a servo-hydraulic test frame. Optical images were taken with a long focal length telescope. The load/deflection response is summarized on Fig. 2(a), where it is compared with an earlier result for a panel with a tetrahedral core (Chiras et al., 2002). The corresponding stress/strain responses are plotted on Fig. 2(b), and compared with curves obtained by simulation (Hyun et al., 2002). The curves measured for the two cores are similar except that the Kagomé topology has a slightly higher peak stress (5.2 MPa relative to 4.8 MPa) and a lower softening rate beyond the peak. Optical images (Fig. 3) affirm that the peak load coincides with the onset of plastic buckling (Hyun et al., 2002), which is noticeably less abrupt than that found for the tetrahedral cores (Chiras et al., 2002): confirming that the

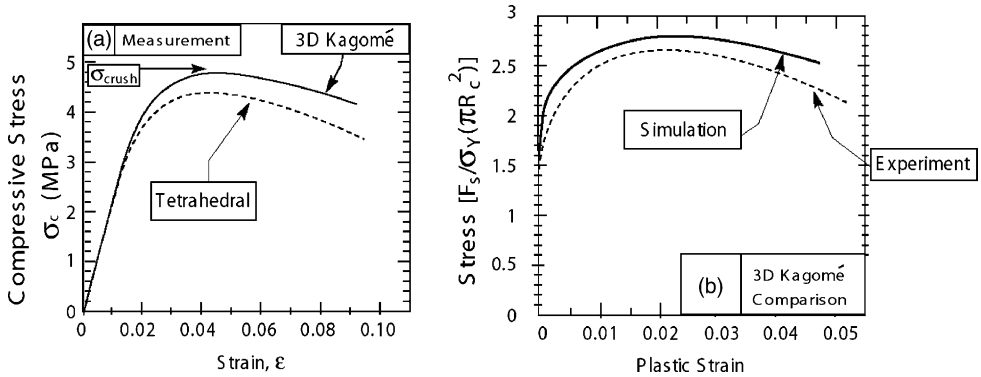

Fig. 2. (a) The compressive response of the 3D Kagomé core relative to that for the tetragonal core (Chiras et al., 2002). (b) The comparison of the compressive stress/strain curve for the 3D Kagomé from (a) with the simulated curve (Hyun et al., 2002).

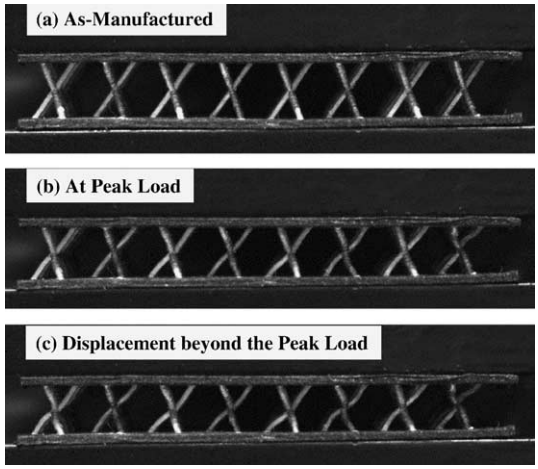

Fig. 3. Optical images obtained at three loads levels during a compression test. Note that extensive plastic buckling occurred beyond the load maximum.

greater load capacity of the Kagomé and its lower softening rate beyond the peak are attributed to its diminished sensitivity to plastic buckling.

4.2. Shear

The shear measurements were performed using an ASTM standard shear test, designed to minimize transverse (compressive) loads (Ashby et al., 2000; ASTM C-273-61, 2002). One panel face was rigidly attached to the stationary actuator of the servo-hydraulic test frame and the other to the cross-head. Optical images were taken with a long focal length telescope. The tests were performed in the three prominent orientations described in the companion article (Hyun et al., 2002) (Fig. 1).

The measured stress/strain curves for the three orientations are compared with the simulated curves on Fig. 4. The isotropy of the Kagomé design is apparent in both the measurements and simulations. The non-dimensional limit load is measured as $F_s/\pi\sigma_Y R^2 \approx 1.4$: the simulations give, $F_s/\pi\sigma_Y R^2 \approx 1.3$ (Hyun et al.,

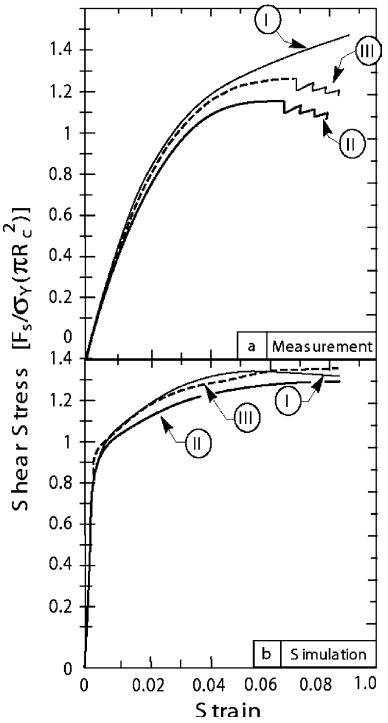

Fig. 4. The shear response of the 3D Kagomé core in the three prominent orientations shown on Fig. 1(b): (a) measurements and (b) simulations.

2002). Beyond the peak, the measurements indicate a softening that does not appear in the simulations, accompanied by a series of load drops. Optical images of regions subject to shear (Fig. 5) indicate that load drops are associated with the rupture of trusses subject to tension. The occurrence of ruptures is attributed to casting imperfections, described below. Note that the load shed by the ruptured trusses redistributes and is supported by neighboring, intact, ligaments. This robustness in the presence of failed ligaments is a key attribute of the Kagomé truss configuration.

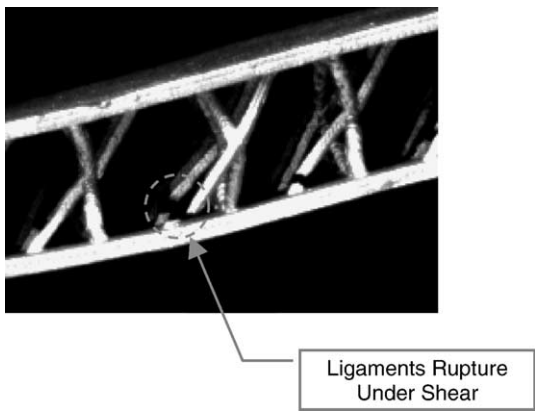

Fig. 5. Optical image showing the rupture of the ligaments that experience tension.

4.3. Panel bending

For bending measurements, 16 mm-wide steel platens with concave external impressions were adhesively bonded to the mid-point of the upper face and to the extremities of the lower face. The loads were applied through the lubricated rollers residing in the concave impressions to assure that the panel rotates upon bending with minimal friction. The load/displacement response is plotted on Fig. 6. The peak load ($P_{max} = 5.07$ kN) is substantially larger than that measured previously for the tetrahedral core ($P_{max} = 3.87$ kN, Fig. 6) (Chiras et al., 2002). The collapse mode is core shear (rather than face yield or indentation). Beyond the peak, the measured loads decrease with associated load drops similar to those found upon shear testing. Optical images (Figs. 5 and 7) affirm that these are attributed to tensile rupture of ligaments in

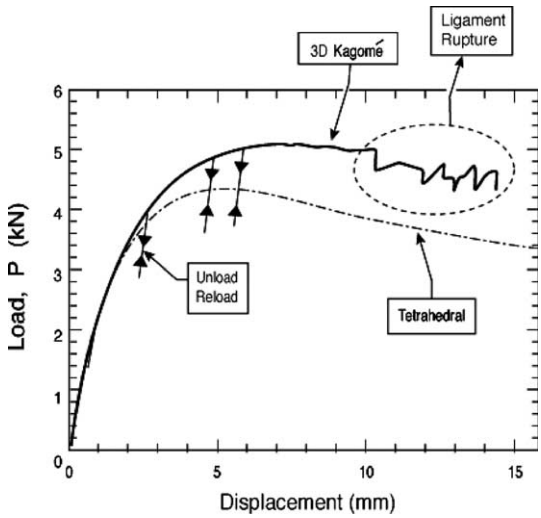

Fig. 6. The three-point bending response of a panel with a 3D Kagomé core compared with that for a tetrahedral core (Chiras et al., 2002).

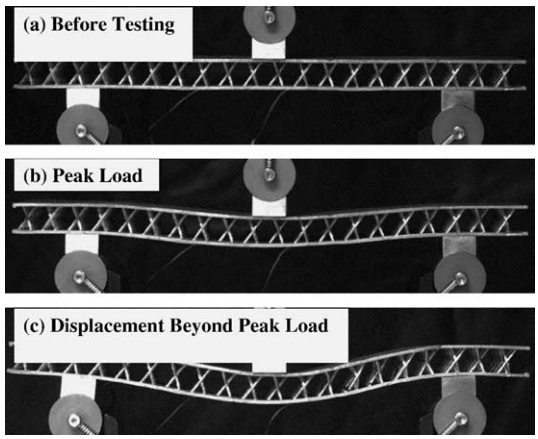

Fig. 7. Optical images taken at different stages of the bending test on the Kagomé panel.

regions subject to shear. The trusses in compression yield but do not buckle. Note that plastic hinges form at the outer support (Fig. 7), because of the relatively large overhang used for the tests (Ashby et al., 2000).

Load/unload cycles (Fig. 6) indicate that the unloading stiffness remains almost unchanged up to the peak load ($S_B \approx 3.25$ MN/m).

4.4. Characterization

Some ruptured ligaments were removed from the panel by electro-discharge machining and the fracture surfaces examined in the scanning electron microscope (SEM). Images of these surfaces (Fig. 8) have revealed that, while the rupture occurred largely by a ductile (hole growth) mechanism, the failure origins contained either casting porosity or cleavage domains. The latter is attributed to intermetallic particles. These imperfections compromise the ductility of the ligaments and cause the premature ruptures noted in the shear and bending tests.

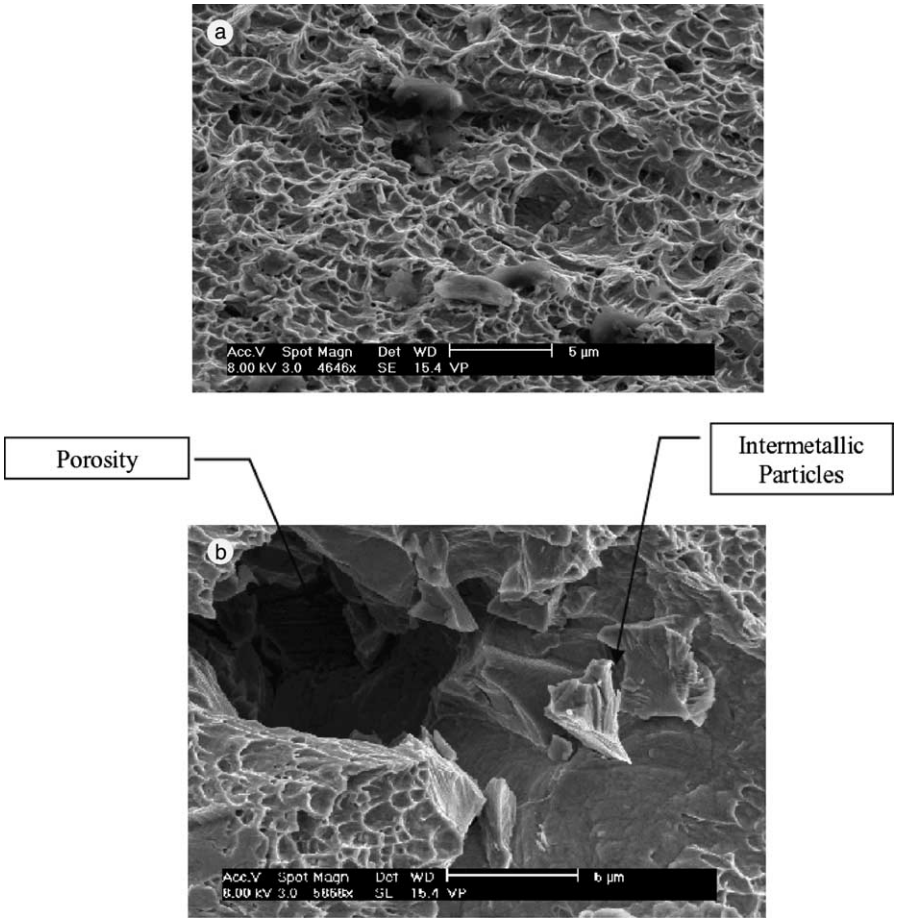

Fig. 8. SEM images of the fracture surfaces of trusses that ruptured during panel bending: (a) ductile dimples on sections that fractured, (b) casting porosity and intermetallic particles.

5. Concluding remark

Experiments performed on sandwich panels with solid face sheets and Kagomé cores have validated the simulations in the companion article (Hyun et al., 2002). The basic finding is that, at the equivalent core density, the Kagomé outperforms tetrahedral and pyramidal cores. The major attributes are its isotropy relative to the competing concepts and the suppression of premature softening caused by plastic buckling. The measurements on the cast panels indicate that imperfections enhance softening modes because of the premature tensile rupture of defective trusses. A wrought alloy fabrication approach (Sypeck and Wadley, 2001) would provide a more robust system.

References

Ashby, F.M., Evans, A.G., Fleck, N.A., Gibson, L.J., Hutchinson, J.W., Wadley, H.G.N., 2000. Metal Foams: A Design Guide. Butterworth–Heinemann, Boston.

C273–00e1, 2002. Standard test method for shear properties of sandwich core materials. ASTM Book of Standards. Vol. 15.03.

Chiras, S., Mumm, D.R., Evans, A.G., Wicks, N., Hutchinson, J.W., Dharmasena, K., Wadley, H.G.N., Fitchter, S., 2002. The structural performance of optimized truss core panels. Int. J. Solids Struct. 39, 4093–4115.

Deshpande, V., Fleck, N.A., 2001. Collapse of truss core sandwich beams in 3-point bending. Int. J. Solids Struct. 38, 6275–6305.

Deshpande, V., Fleck, N.A., Ashby, M.F., 2001. Effective properties of the octet-truss lattice material. J. Mech. Phys. Solids 49, 1747–1769.

Evans, A.G., 2001. Lightweight materials and structures. Mater. Res. Bull. 26, 790–797.

Evans, A.G., Hutchinson, J.W., Ashby, M.F., 1998. Multifunctionality of cellular metal systems. Prog. Mater. Sci. 43, 172–221.

Evans, A.G., Hutchinson, J.W., Fleck, N.A., Ashby, M.F., Wadley, H.G.N., 2001. The topological design of multifunctional cellular metals. Prog. Mater. Sci. 46, 311–327.

Hyun, S., Karlsson, A.M., Torquato, S., Evans, A.G., 2002. Simulated properties of Kagomé and tetragonal truss core panels, Int. J. Solids Struct., in press.

Sypeck, D.J., Wadley, H.N.G., 2001. Cellular metal truss core sandwich structures. In: Banhart, J., Ashby, M.F., Fleck, N.A. (Eds.), Cellular Metals and Metal Foaming Technology. MIT-Verlag, pp. 381–386.

Wallach, J.C., Gibson, L.G., 2001. Mechanical behavior of a three-dimensional truss material. Int. J. Solids Struct. 38, 7181–7196.

Wicks, N., Hutchinson, J.W., 2001. Optimal truss plates. Int. J. Solids Struct. 38, 5165–5183.